



Shahid Chamran  
University of Ahvaz

# Journal of Applied and Computational Mechanics



Research Paper

## Study of Hybrid Composite Joints with Thin-ply-reinforced Adherends under High-rate and Impact Loadings

Farin Ramezani<sup>1</sup>, Ricardo J.C. Carbas<sup>1,2</sup>, Eduardo A.S. Marques<sup>2</sup>, Lucas F.M. da Silva<sup>2</sup>

<sup>1</sup>Instituto de Ciência e Inovação Em Engenharia Mecânica e Engenharia Industrial (INEGI), Rua Dr. Roberto Frias, 4200-465 Porto, Portugal, Email: farinramezani@gmail.com

<sup>2</sup>Departamento de Engenharia Mecânica, Faculdade de Engenharia (FEUP), Universidade Do Porto, Rua Dr. Roberto Frias, 4200-465 Porto, Portugal, Email: rcarbas@fe.up.pt (R.J.C.C.); emarques@fe.up.pt (E.A.S.M.); lucas@fe.up.pt (L.F.M.S)

Received July 04 2023; Revised October 31 2023; Accepted for publication October 31 2023.

Corresponding author: R.J.C. Carbas (rcarbas@fe.up.pt)

© 2023 Published by Shahid Chamran University of Ahvaz

**Abstract.** This research aims to examine the tensile strength of a hybrid composite laminate reinforced by thin-ply when used as an adherend in bonded single lap joints subjected to high-rate and impact loading. Two different composites, namely Texpreg HS 160 T700 and NTPT-TP415, are employed as the conventional and thin-ply composites, respectively. The study considers three configurations: a conventional composite, a thin-ply, and a hybrid single lap joint. Numerical models of the configurations are developed to provide insight into failure mechanisms and the initiation of damage. The results indicate a significant increase in tensile strength for the hybrid joints over the conventional and thin-ply joints, due to the mitigation of stress concentrations. Overall, this study demonstrates the potential of hybrid laminates for improving the performance of composite joints under high-rate loading and impact conditions.

**Keywords:** Composite joints, thin-ply, single lap joints, high-rate loading, impact loading.

### 1. Introduction

In composites, two primary components are involved: the matrix and the reinforcement. The matrix offers the material cohesion, while the reinforcement, usually in fibre form, provides strength and stiffness [1]. The utilization of carbon fibre-reinforced polymer (CFRP) materials is experiencing continuous growth [2-6] in various industries, including those manufacturing vehicle structures, sporting goods, etc [7]. However, despite their numerous benefits, bonding composites faces a critical issue, arising from the likelihood of the presence of defects in the adhesive layer, taking the form of voids or debonding [8, 9]. Generally, studies have shown that the presence of an imperfection such as a void or a debond in the overlap region will cause an increase in the value of interfacial shear stress in the regions close to the imperfection. This increase depends on the length and, especially, location of the defect [10, 11]. On the other hand, the significant disparity between the strength of the reinforcement and the matrix means that the loads applied perpendicularly to the reinforcement are predominantly borne solely by the low-strength matrix, resulting in the development of matrix cracks and subsequent delamination. Delamination can cause rapid degradation in the mechanical performance of the structure and lead to premature failure [12-16]. Several research studies have explored methods to modify joints in order to mitigate delamination in adhesively bonded composite joints [17-29]. However, the implementation of these methods usually necessitates at least one extra production step, which, in turn, leads to increased production costs. Moreover, the intricate nature of these techniques often constrains their practical application [30, 31].

The spread-tow technique has emerged as a result of recent advances in composite manufacturing technology [32] which results in plies with a more homogeneous fibre distribution and smaller resin-rich regions [33], allowing achieve a dry ply thickness as low as 0.02 mm. Typically, plies with a thickness of less than 100  $\mu\text{m}$  are referred to as thin-ply [34]. Reducing the thickness of an individual layer expands the number of feasible layers, increasing the degrees of freedom in design [35], while it also results in a larger number of interfaces in thin-ply laminates, lowering the shear stresses [35, 36]. Furthermore, thin-ply laminates are recognized for their capacity to postpone the initiation of matrix damage mechanisms, suppress transverse microcracking [32] and free edge delamination [35, 37] for static, fatigue, and impact loadings. Due to their exceptional resistance to damage and delamination, thin-ply laminates could potentially display elevated interlaminar shear properties [38] and strain energy [39] compared to conventional plies. Consequently, thinner composite plies are recognized to possess superior in situ transverse strength [36]. Use of thin-ply is currently regarded as a promising strategy to enhance the performance of adhesively bonded CFRP structures, primarily because of the capability to improve the off-axis properties of composites and delay the onset of delamination [39]. Additionally, research has indicated that the incorporation of thin-ply in a structural joint results in a shift of the damage location in the composite from the adhesive interface towards the mid-thickness of the adherends [39], mainly due to the in-situ effect [40].



In a previous study conducted by the authors [41], it was demonstrated that substituting conventional composite layers with thin-ply layers in the adherends of a single lap joint can significantly enhance the strength of the composite joint, as well as improve the failure mode (by reducing delamination) under static loads. The authors attribute this change to the improved ductility of the laminate, which can delay delamination [42]. Moreover, experimental observation clearly demonstrated that the presence of thin-ply acts as a barrier against crack propagation.

In summary, the study aims to investigate the performance of a hybrid (25% thin-ply) composite single lap joint reinforced with thin-ply layers under high-rate and impact loads. Two types of materials were considered to create the hybrid (25% thin-ply) joint: a conventional composite (HS 160 T700) and a thin-ply material (NTPT-TP415). Numerical models were also created using cohesive zone modelling to accurately replicate the experimentally determined failure processes.

## 2. Experimental Details

### 2.1. Adhesive

The adhesive used in this work was an epoxy structural adhesive, supplied in film form, with the commercial reference Scotch Weld AF 163-2k (3M, Saint Paul, Minnesota, USA) and the following properties: Young's modulus ( $E$ )=1.5 GPa, shear modulus ( $G$ )=0.6 GPa, tensile strength ( $\sigma$ )=46.9 MPa, shear strength ( $\tau$ )=46.8 MPa, fracture energy ( $G_{IC}$ = 4.05 and  $G_{IIC}$ =9.77 N/mm) [43]. Morgado et al. [43] characterized the mechanical properties of AF 163-2k is under quasi-static (1 mm/min) and impact loading conditions (3 m/s). The mechanical properties at high-rate (0.1 m/s) and impact loading (2 m/sec) were calculated using a linear extrapolation. The adhesive was cured following the manufacturer's recommendations, at 130°C for 2 hours.

### 2.2. Adherend

#### 2.2.1. Conventional Composite

The materials used in the studied configurations were selected in order to be representative of a possible application within the aerospace sector. Accordingly, a unidirectional prepreg carbon-epoxy composite with a ply thickness of 0.15 mm was selected, with the commercial reference "Texipreg HS 160 T700" (Seal Spa, Legnano, Italy) and the following properties: Young's modulus ( $E_1$ =109.0 and  $E_2$ =8.8 GPa), shear modulus ( $G_{12}$ =4.3 and  $G_{13}$ =3.2 GPa), fracture energy ( $G_{IC}$ = 0.6 and  $G_{IIC}$ =1.2 N/mm) [44, 45]. Morgado et al. [46] presented the mechanical properties of the cured prepreg under static (1mm/min) and impact loading conditions (3 m/s). The mechanical properties at high-rate (0.1 m/s) and impact loading (2 m/sec) were calculated using a linear extrapolation.

#### 2.2.2. Thin-Ply

A unidirectional 0° oriented carbon-epoxy prepreg composite with a ply thickness of 0.075mm was selected for use in this work, serving as the thin-ply material. This material has the commercial reference "NTPT-TP415" (North thin-ply technology, Poland) and the following properties: Young's modulus ( $E_1$ =101.7 and  $E_2$ =5.7 GPa), shear modulus ( $G_{12}$ =3.0 and  $G_{13}$ =3.0 GPa), fracture energy ( $G_{IC}$ = 0.7 and  $G_{IIC}$ =0.8 N/mm) [47]. The mechanical properties at high-rate (0.1 m/s) and impact loading (2 m/sec) were calculated using a linear extrapolation.

### 2.3. Single Lap Joint Manufacturing

The manufacturing process for the single lap joints involved layer-by-layer stacking of conventional composite and thin-ply prepregs to achieve the desired adherend thickness of 3.6mm. The reference conventional composite adherends consisted of 24 layers, while the thin-ply adherends consisted of 48 layers. For the hybrid adherends (25% thin-ply), 6 plies of conventional composite were replaced by 12 plies of thin-ply on the adherend tops (6 layers of thin-ply on each adherend top), resulting in a 25% thin-ply composition. An additional layer of adhesive was then applied between the adherends. A mould was used to ensure the thickness of the adherends and adhesive. To facilitate easy detachment of the specimens from the mould after curing, a release agent was applied. The effect of curing sequence on the mechanical properties of the joint was investigated by comparing the performance of joints where the composite and the adhesive were cured together (co-cured) with the joints where curing occurred separately. It was found that, for the AF163-2k adhesive used in this study, the curing sequence had no significant impact on the mechanical properties of the joint. As a result, a one-step curing process was selected as the preferred method of manufacturing, allowing for a reduction in both the manufacturing time and energy consumption. The joint was cured at 130°C for 2 hours following the manufacturer's recommended procedure. Single lap joints (SLJs) were manufactured with the geometry shown in Fig. 1.

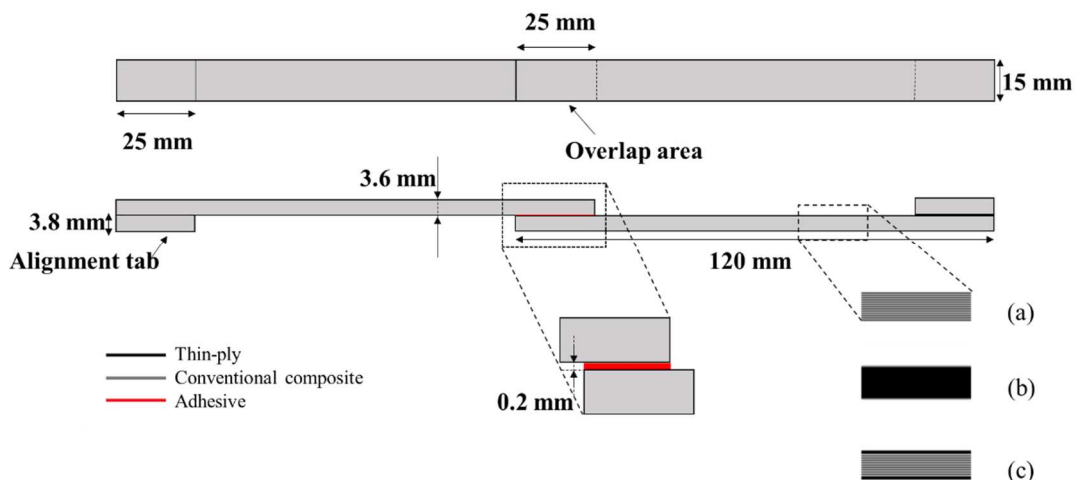


Fig. 1. Schematic design of single lap joint with (a) conventional composite, (b) thin-ply and, (c) hybrid (25% thin-ply) adherends.



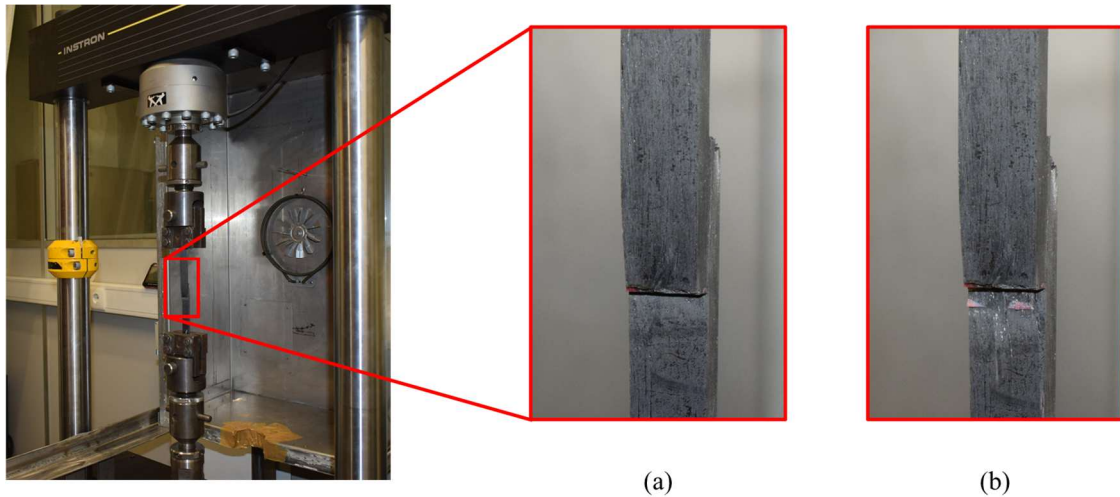


Fig. 2. (a) Intact, (b) failed specimen in servo hydraulic testing machine.

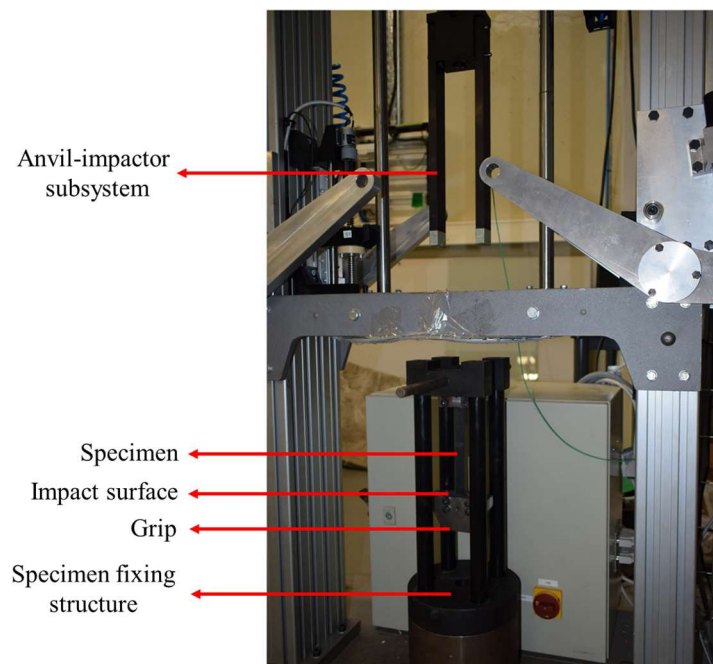


Fig. 3. Drop wight machine.

#### 2.4. Testing Condition

The SLJs were tested at two different constant crosshead speeds of 0.1 and 2 m/sec known as the high-rate and impact loading condition. An Instron 8801 servo hydraulic testing machine with a load cell of 100 kN for the high-rate loading. Figure 2 provides an image of the intact and damaged specimen in the servo hydraulic testing machine. An in-house developed drop-weight testing machine was used to carry out impact tests on the specimens [48]. This machine grips the upper part adherend, leaving the lower portion free. A mass is then dropped from a specific height, causing an impact on the lower part of the grip and loading the specimen in tension-shear. The impact velocity is determined by the drop height, which follows the principle of energy conservation. For the impact tests in this study, a 50 kg mass and an impact velocity of 2 m/s were chosen, resulting in an impact energy of 100 J. Figure 3 presents an image of an intact specimen in the drop weight testing machine. It has to be mentioned that the rising time of the impactor from the stationary station was about three seconds, considering the speed, mass, and stationary state mentioned above. All tests were performed under laboratory ambient conditions (room temperature of 24°C, relative humidity of 55%). Four repetitions were performed for each configuration under analysis.

### 3. Experimental Result

#### 3.1. High-Rate Loading

Figure 4 illustrates representative experimentally obtained load-displacement curves for the studied configurations under high-rate loading. The hybrid (25% thin-ply) joint presented the highest failure load, with around a 25% increase in joint strength compared to the reference conventional composite configuration. Figure 5 provides representative images of the failure surface for all configurations. As seen, delamination is the dominant failure mode observed in all tested composite single lap joint configurations.



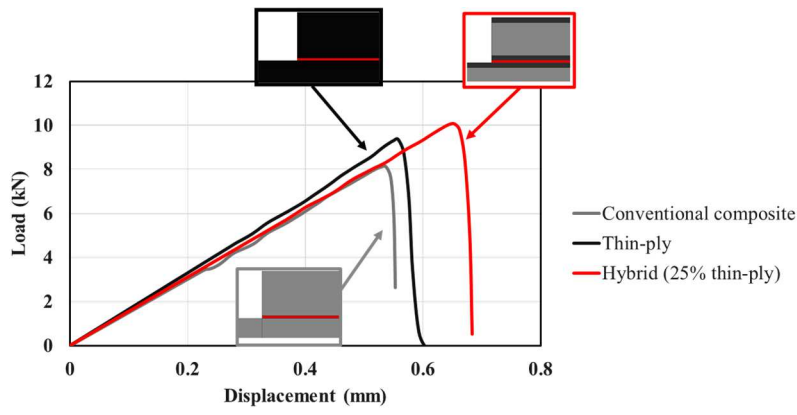


Fig. 4. Representative load-displacement curves for reference conventional composite, thin-ply and hybrid (25% thin-ply) joint under high-rate loading.

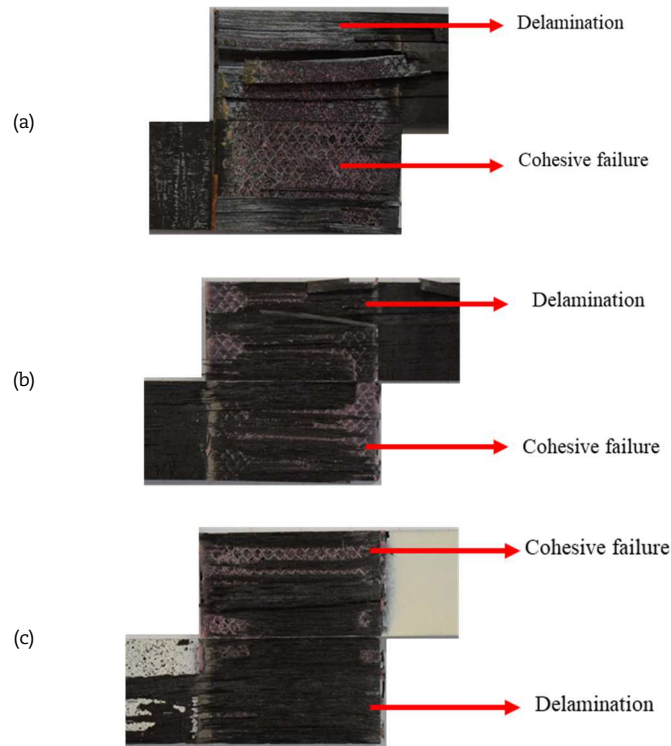


Fig. 5. Representative images of failure surface of (a) reference conventional composite, (b) thin-ply and, (c) hybrid (25% thin-ply) joint under high-rate loading.

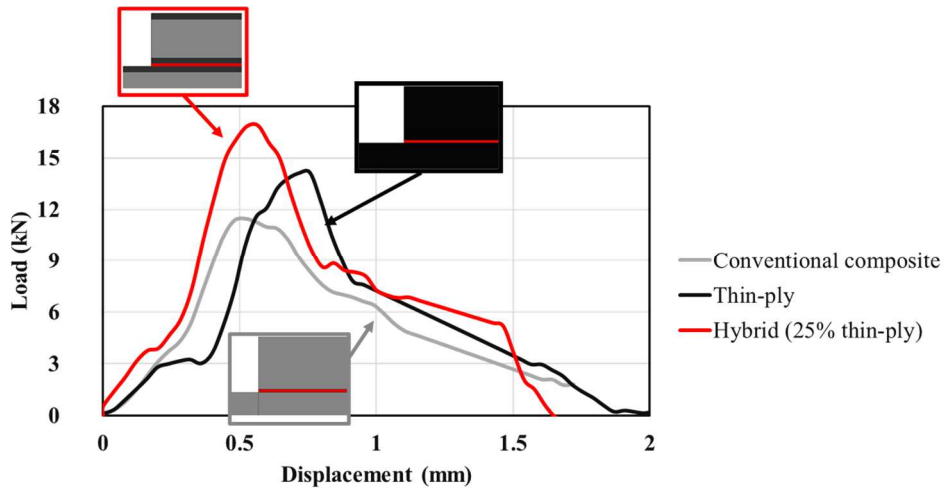


Fig. 6. Representative load-displacement curves for reference conventional composite, thin-ply and hybrid (25% thin-ply) joint under impact loading.



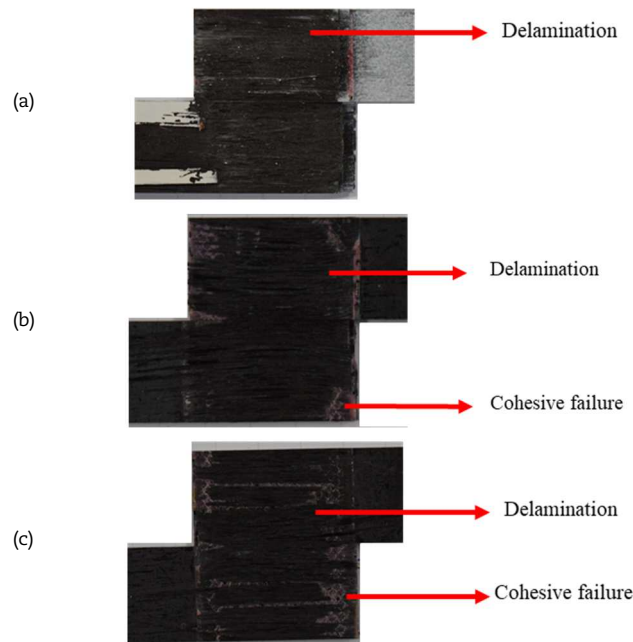


Fig. 7. Representative images of failure surface of (a) reference conventional composite, (b) thin-ply and, (c) hybrid (25% thin-ply) joint under impact loading.

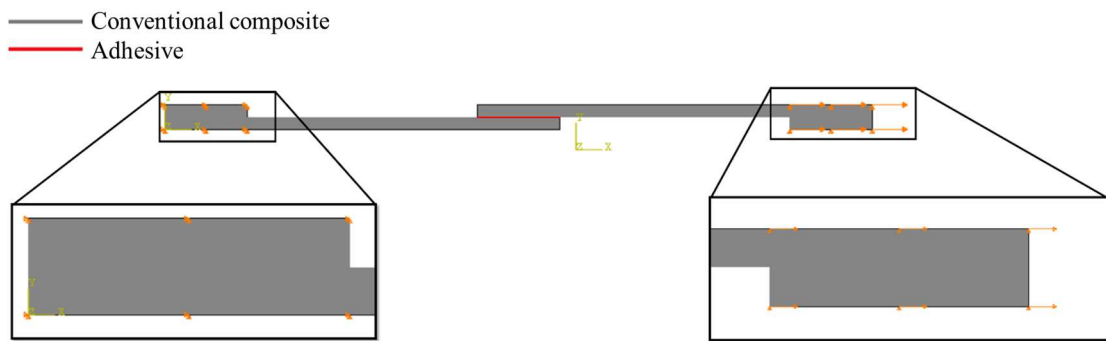


Fig. 8. Boundary condition of simulated conventional composite single lap joint.

### 3.2. Impact Loading

Figure 6 provides representative load-displacement curves for the configurations tested experimentally under impact loading. The hybrid (25% thin-ply) joint presented the highest failure load, with around an 50% increase in joint strength compared to the reference conventional composite configuration. Figure 7 provides representative images of the failure surface for all configurations. For the reference joints with conventional composite full delamination was observed. In contrast, for reference joints with thin-ply and the hybrid (25% thin-ply) joints, partial cohesive failure was also observed in addition to the most dominant delamination failure mode.

## 4. Numerical Study

For high-rate and impact loading, a 2D explicit and 3D implicit dynamically loaded model was employed, using the Abaqus/CAE 6.14-2 commercial finite element package respectively. The boundary conditions were established as depicted in Fig. 8, where the left end of the joint was fixed and an amplitude of displacement was applied to the right end to mimic the dynamic loading conditions. A displacement of 1 and 2 mm was applied to the numerical models as described above for high-rate and impact loading respectively. The mention displacement was chosen based on experimental results in order to make sure the failure occurred. In order to simulate the high-rate and impact loading an amplitude of 0.01 and 0.001 was applied to the numerical models, respectively.

To model the behaviour of the adhesive and simulate damage evolution, a cohesive zone model (CZM) was employed, using four node cohesive quadrilateral elements. Non-linear geometrical effects were considered, and solid cohesive elements were used to represent damage evolution (damage initiation and propagation), following a traction-separation law. CZM was also introduced into the composite material to model delamination, and the interlaminar cohesive element layers (conventional composite or thin-ply) were placed between elastic homogeneous sections [49].

The mechanical properties assigned to these numerical models are shown in Fig. 9, with CZM layers placed at different distances for high-rate loading and impact loading. The distance from the interface of the adherend and adhesive layer varied depending on the joint configuration and loading type. The CZM layers were placed at a distance of 0.17, 0.15, and 0.28 mm from the interface of the adherend and adhesive layer for the conventional composite, thin-ply, and hybrid (25% thin-ply) joints under high-rate loading, respectively. Similarly, for impact loading, CZM layers were placed at a distance of 0.20, 0.30, and 0.45 mm from the interface of the adherend and adhesive layer for the mentioned configurations. This distance roughly corresponded to the experimentally measured distance of the delamination plane from the adhesive layer. The thickness of the cohesive layer matched the thickness of one equivalent composite ply (0.075 mm for thin-ply and 0.15 mm for the conventional composite).



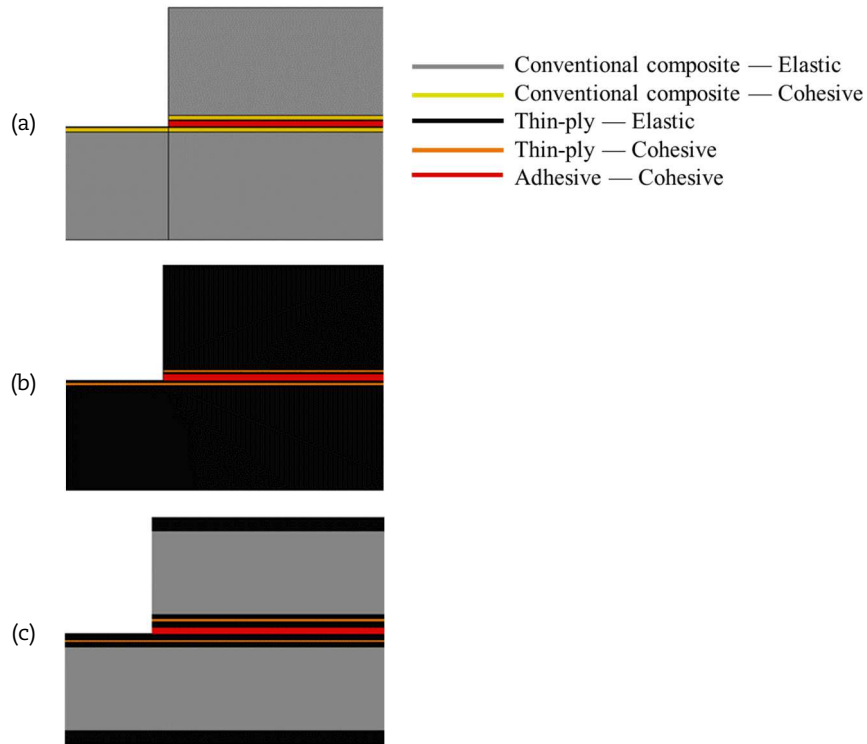


Fig. 9. Assigned mechanical properties for (a) conventional composite, (b) thin-ply, and (c) hybrid (25% thin-ply) joints for high-rate loading.

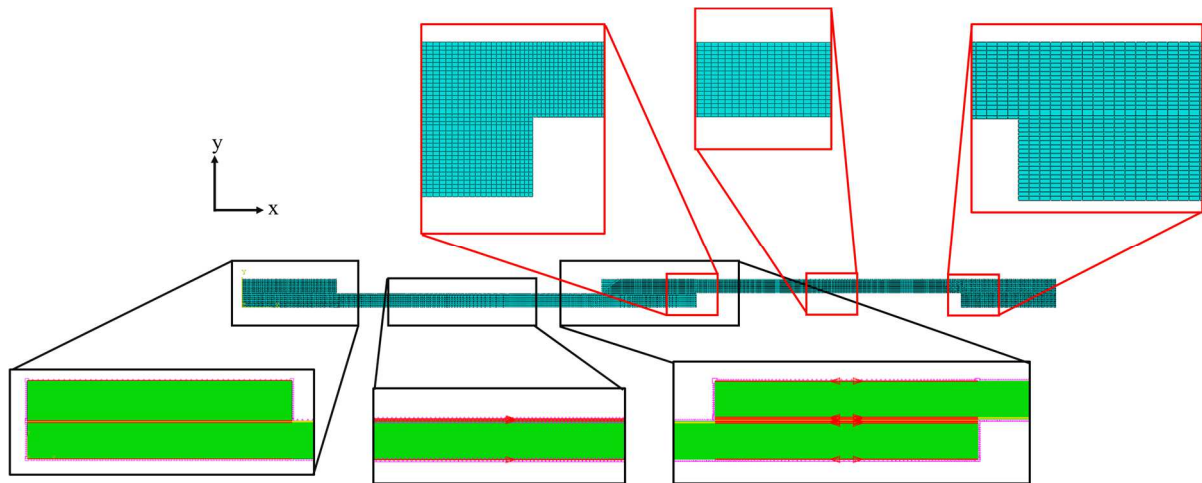


Fig. 10. Mesh distributions for single-lap joint.

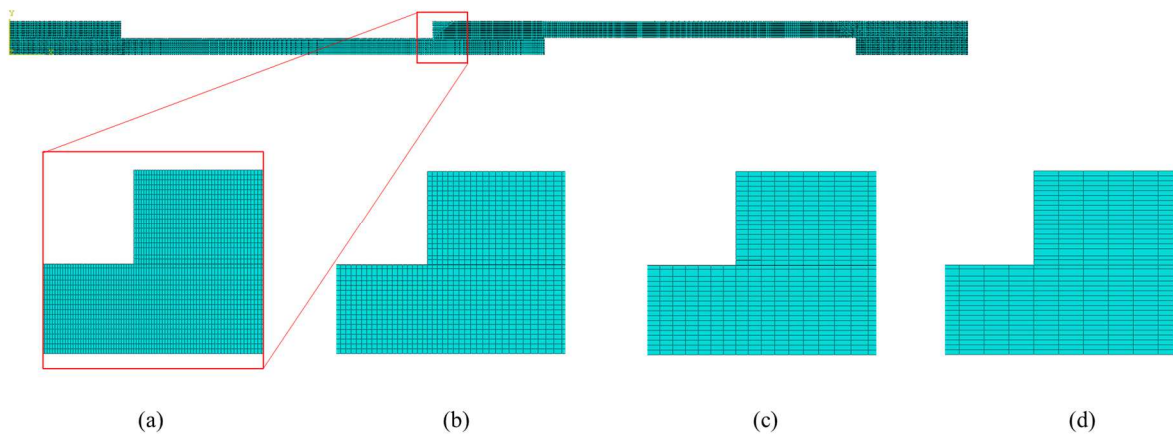


Fig. 11. Mesh distributions for single-lap joints with minimum and maximum mesh size of (a) 0.1 and 0.2 mm, (b) 0.2 and 0.5 mm, (c) 0.5 and 1 mm and (d) 1 mm, respectively.



Additionally, a mesh convergence study was performed for the reference conventional composite single lap joint under high-rate loading in order to study the effect of mesh size on the numerically obtained failure load. The mesh size in the thickness direction (y direction-see Fig. 10) is restricted to the thickness of the cohesive layer. This is because a cohesive model zone analysis allows the use of only a row of cohesive elements in the cohesive layer. Therefore, elements size of 0.2 mm (thickness of the cohesive layer) was considered for the thickness direction. However, the effect of mesh size in the x direction was studied. Double and single biased mesh distributions were considered in the x direction (see Fig. 10) for the bondline and the adherends, respectively. Accordingly, the minimum mesh size of 0.1, 0.2, 0.5 and 1 mm was considered to study the effect of mesh size on the numerical result. The detailed mesh size was presented in Fig. 11. According to the results presented in Fig. 12, the minimum mesh size of 0.2 could validate the finite element findings for the purpose of comparison with the experimental results additional to minimizing the computational cost of the numerical models. Consequently, the minimum and maximum sizes for the mesh were considered 0.2 and 0.5 mm respectively for the bondline and the adherends. End tabs were meshed uniformly with a size of 0.5 mm in the x direction, and the mesh was uniform through the thickness (y direction) with a size of 0.2 mm for all components. The same mesh size was used for all numerical models. The resulting mesh consisted of approximately 15,000 elements for 2D models and 75,000 elements for 3D models.

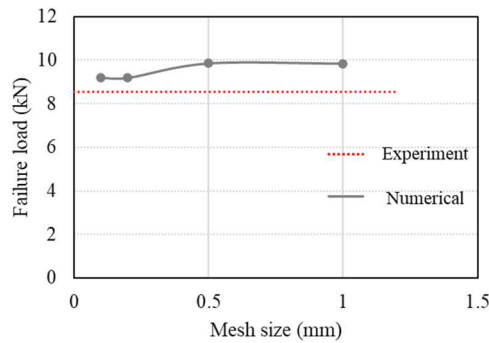


Fig. 12. Effect of mesh size on the numerically obtained failure load in comparison with the experimentally obtained result for the reference conventional composite single lap joint under high-rate loading.

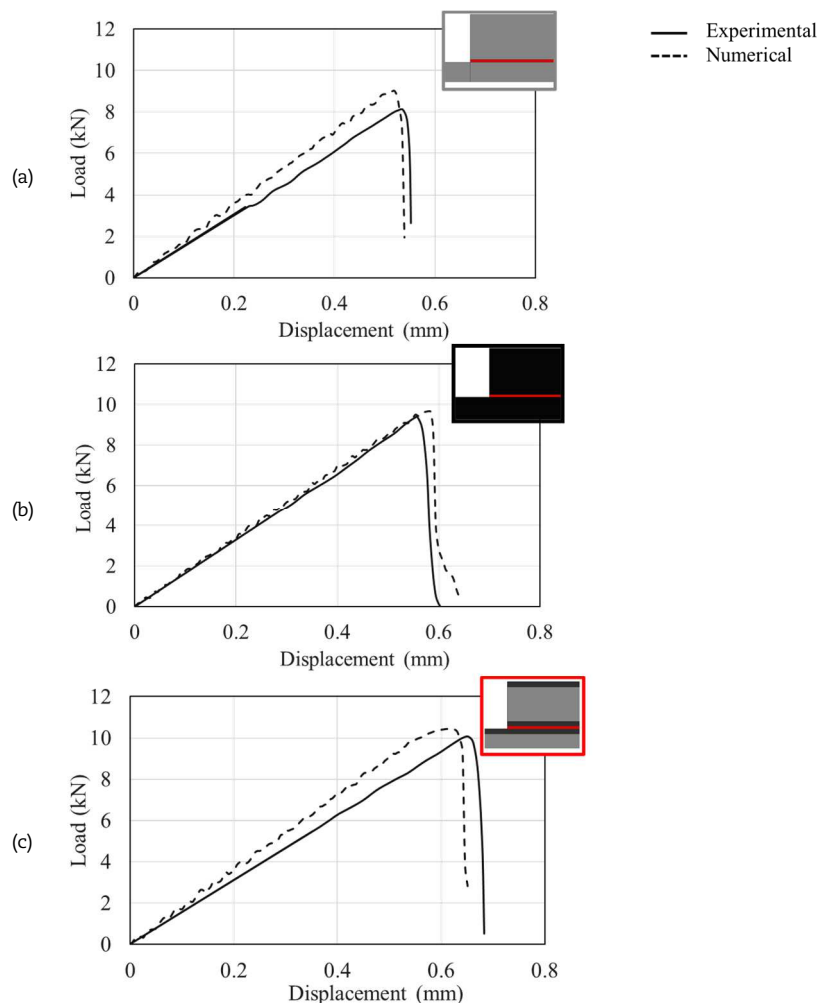


Fig. 13. Comparison of numerically obtained load-displacement curves for (a) conventional composite, (b) thin-ply and, (c) hybrid (25% thin-ply) joint with the representative experimental results under high-rate loading.



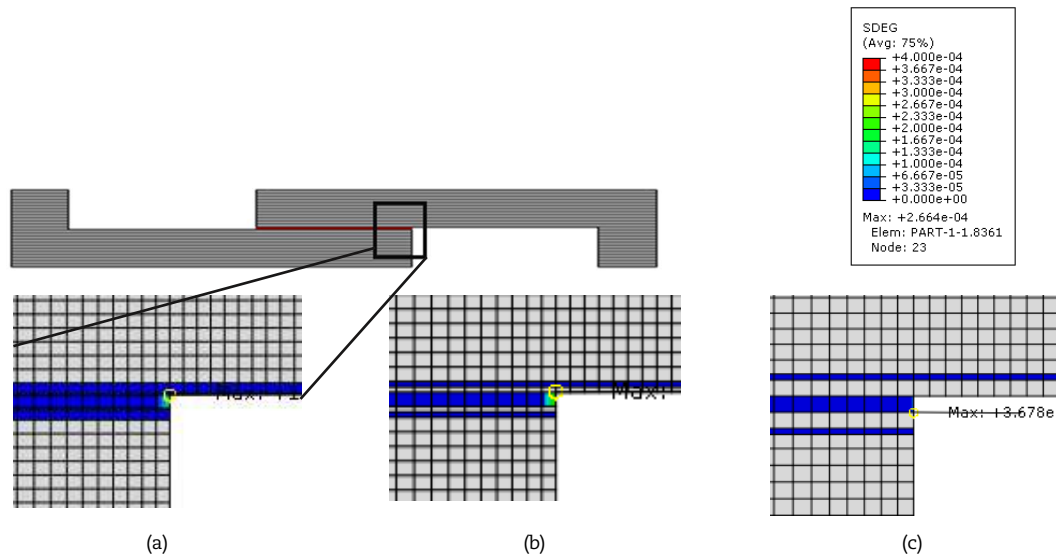


Fig. 14. SDEG at damage initiation for (a) conventional composite, (b) thin-ply and (c) hybrid (25% thin-ply) joint under high-rate loading (equivalent load for each configuration is 6.8, 6.9, and 7.0 kN, respectively).

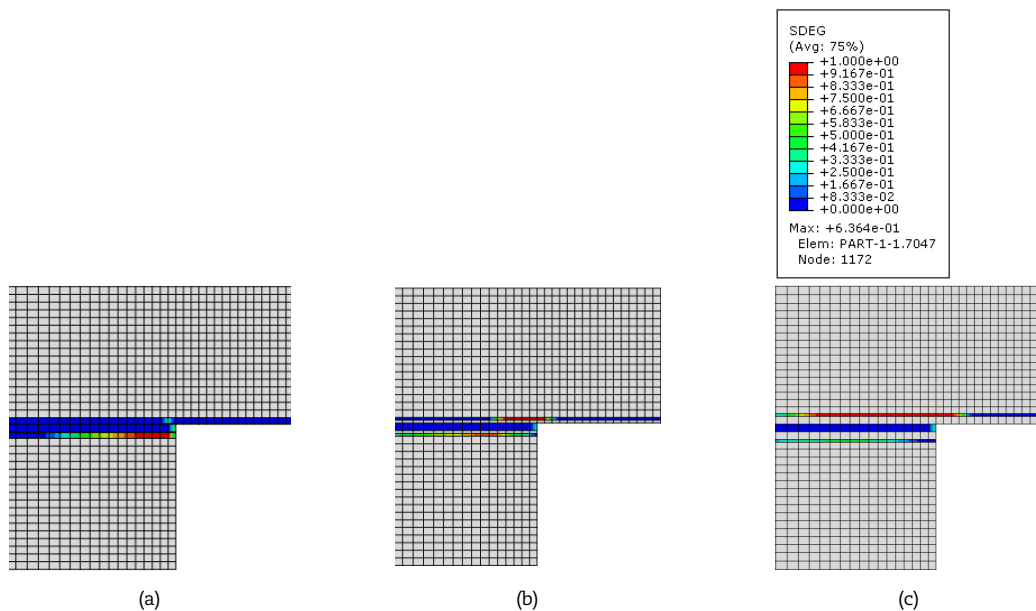


Fig. 15. SDEG at corresponding failure load for (a) conventional composite, (b) thin-ply and (c) hybrid (25% thin-ply) joint under high-rate loading.

#### 4.1. High-Rate Loading

The load-displacement curves obtained numerically for all configurations under high-rate loading are presented in Fig. 13. As seen, there is a good match between the numerical and the experimentally obtained load-displacement curves. Figure 14 illustrates the damage initiation for each configuration. The presented area is shown within by the black square in single lap joint. The equivalent load for damage initiation (load in which damage initiation occurs) for the reference conventional composite, reference thin-ply and the hybrid (25% thin-ply) single lap joints was 6.8, 6.9, and 7.0 kN respectively. It should be mentioned that the damage initiation occurs at a higher level of load for the hybrid (25% thin-ply) compared to the both conventional composite and thin-ply reference single lap joint. Additionally, as seen in Fig. 14, the stiffness degradation was more objective in the both conventional composite and thin-ply reference single lap joint compared to the hybrid (25% thin-ply). However, damage initiation was shown to occur in the adhesive layer for all configurations. Figure 15 illustrates the damage state for all configurations at their corresponding failure load. As seen, the final failure mode is known to be delamination for all configurations which is in line with the experimentally obtained result.

#### 4.2. Impact-Loading

The numerical load-displacement curves, obtained for all configurations under impact loading, are presented in Fig. 16 and compared with the equivalent experimentally obtained load-displacement for each configuration. Figure 17 illustrates the damage initiation for each configuration. The presented area is shown within the black square in the single lap joint. The equivalent load of damage initiation for the reference conventional composite, reference thin-ply and the hybrid (25% thin-ply) single lap joints were 6.7, 5.3, and 5.6 kN respectively which was cited in the adhesive layer. However, the final failure was illustrated as delamination as seen in Fig. 18.





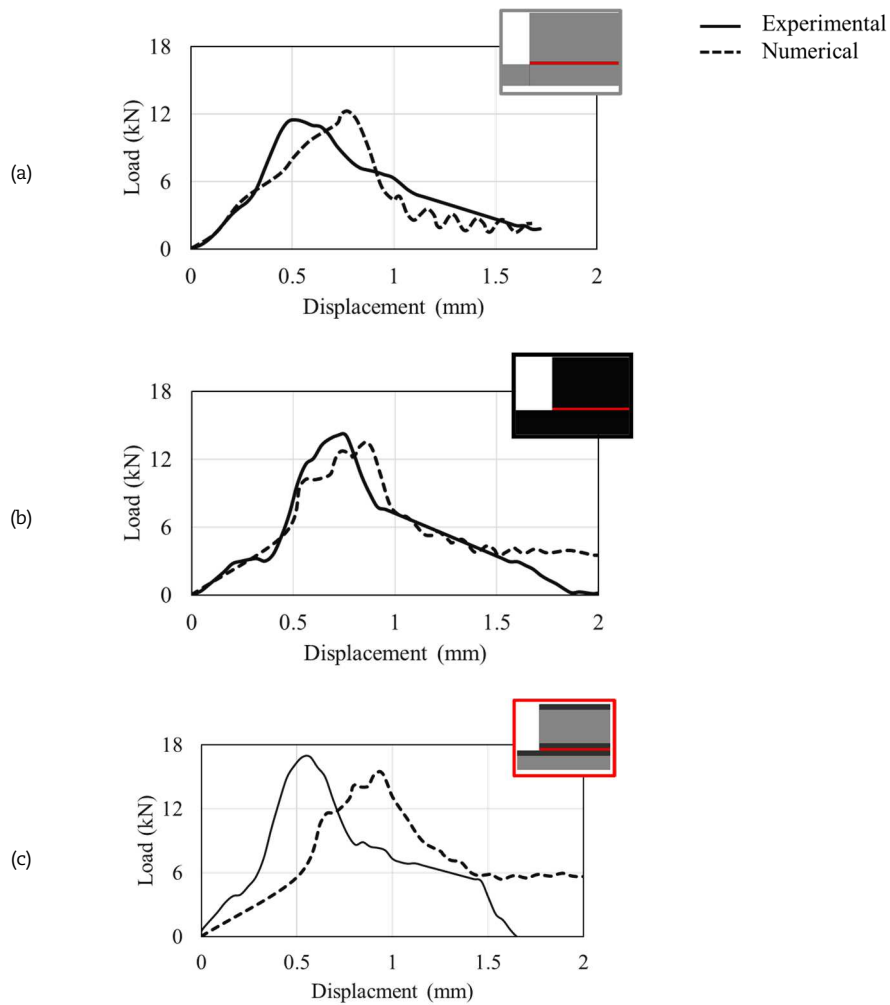


Fig. 16. Comparison of numerically obtained load-displacement curves for (a) conventional composite, (b) thin-ply and, (c) hybrid (25% thin-ply) joint with the representative experimental results under impact loading.

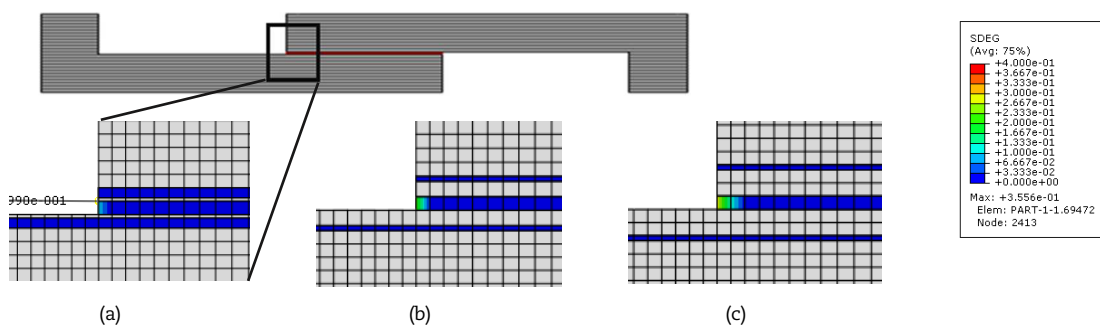


Fig. 17. SDEG at damage initiation for (a) conventional composite, (b) thin-ply and (c) hybrid (25% thin-ply) joint under impact loading (equivalent load for each configuration is 6.7, 5.3 and 5.6 kN, respectively).

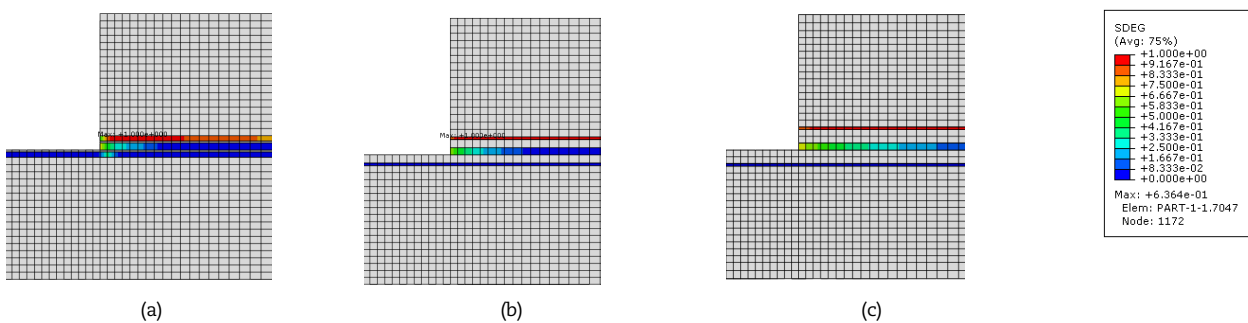


Fig. 18. SDEG at corresponding failure load for (a) conventional composite, (b) thin-ply and (c) hybrid (25% thin-ply) joint under impact loading.



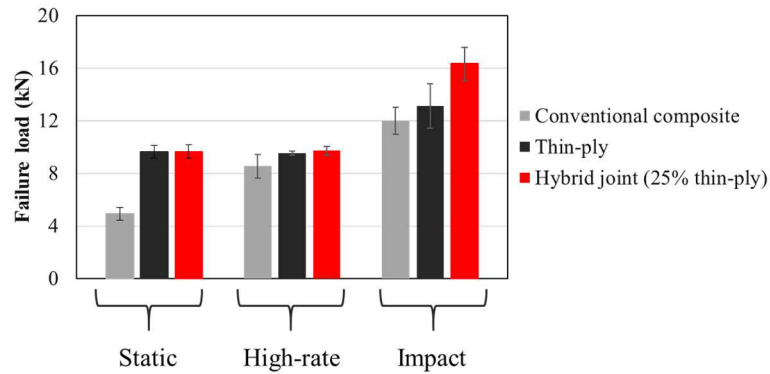


Fig. 19. Comparison of the experimentally obtained failure load for conventional composite, thin-ply and hybrid (25% thin-ply) single lap joint under high-rate and impact loading with ones obtained statically loaded.

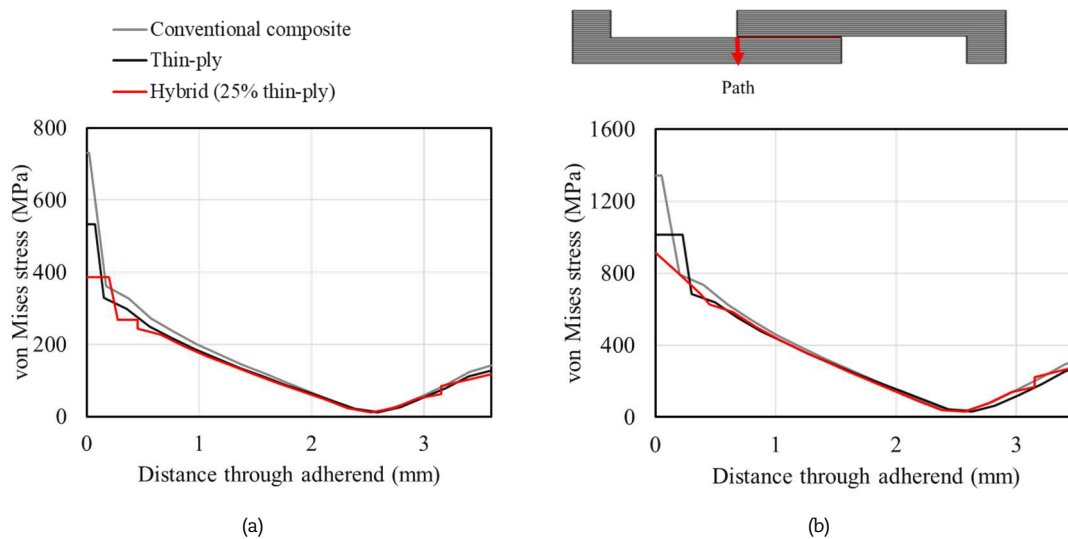


Fig. 20. von Mises stress distribution through the adherend thickness (a) under high-rate loading at 5 kN and (b) under impact loading at 11.5 kN.

## 5. Discussion

The use of hybrid (25% thin-ply) composite joints reinforcement with thin-ply has demonstrated a remarkable enhancement in the tensile strength of up to 90%, compared to conventional composite joints under static loading conditions. This study conducted an investigation of the performance of hybrid joints incorporating 25% thin-ply under high-rate and impact loading. Figure 19, illustrate the average failure load of conventional composite joints, thin-ply joints, and hybrid (25% thin-ply) single lap joints under static, high-rate, and impact loading conditions. These findings suggest that hybrid (25% thin-ply) single lap joints exhibit superior tensile strength not only under static loading but also under high-rate and impact loading conditions compared to conventional composite joints. This is mainly due to higher ductility conferred to the material by the presence of thin-ply [42]. Thin-ply materials are also known to have higher resistance to crack propagation which is mainly know to be due to the more uniform fibre distribution and less resin-rich and fibre-rich area in the thin-ply [42]. In the previous study [41], it was shown that for hybrid (25% thin-ply) single lap joints more limited amount of delamination was obtained compared to the reference ones under static loading. As seen in Fig 19 the thin-ply and hybrid (25% thin-ply) display almost the same strength under both static and high-rate loading (about 10 kN). This is while a considerable increase was observed in the joint strength for the reference thin-ply when increasing the cross-head speed up to 2 m/sec. It could be concluded that thin-ply materials preform even better under impact loading. Therefor when combining thin-ply with the conventional composite which is known to have more brittle behavior compared to the thin-ply (higher strength but premature failure is expected for the conventional composite), tensile resistance of the hybrid composite joint could be increased compared to both reference conventional composite and thin-ply single lap joints. However, it should be noted that the manufacturing process for the former is less expensive and time-consuming. In addition, all configurations have shown delamination to be the dominant failure mode, both under high-rate and impact loads. The numerical analysis and study revealed that damage initiation takes place in the adhesive layer and propagates through the adherend as delamination, which aligns with the experimental observations.

Since delamination is the predominant failure mode across all configurations, the equivalent von Mises stress was analysed through the adherend thickness at 5 and 11.5 kN for the high-rate and impact models respectively in order to gain a deeper understanding of the mechanism responsible for the increased tensile strength of hybrid (25% thin-ply) single lap joints. The path for which the von Mises stress was obtained was shown in Fig. 20. As depicted in Fig. 20, the composite adherends of thin-ply and hybrid (25% thin-ply) joints were found to experience lower levels of equivalent von Mises stress at a constant load level during high-rate and impact loading compared to the reference conventional composite single-lap joint. This could be explained by the ductile behavior of the thin-ply composite compared to the conventional one [42] which induces a lower level of stress to the adherends. This study highlights that hybrid (25% thin-ply) composite joints have the potential to be an effective solution for increasing structural integrity under different loading conditions.



## 6. Conclusion

The performance of hybrid (25% thin-ply) composite single lap joints under high-rate and impact loading was studied and compared to the static response. Overall, hybrid (25% thin-ply) composite joints were found to be a promising solution for enhancing the structural strength. In conclusion, it was observed that:

- The use of hybrid (25% thin-ply) composite joints reinforced with thin-ply exhibit higher tensile strength than conventional composite joints under all loading conditions.
- Delamination is the dominant failure mode across all configurations for high-rate and impact loads.
- The developed numerical models, using cohesive zone modelling, were found to be in a good agreement with the experimental results for both high-rate and impact conditions.
- Numerical analysis revealed that the damage initiates in the adhesive layer and propagates in the composite adherends as delamination which is in line with the experimental observation.
- The analysis of equivalent von Mises stress through the adherend thickness at a constant load revealed that hybrid (25% thin-ply) joints experience lower stress levels during high-rate and impact loading.

## Author Contributions

Investigation, F. Ramezani; Writing—original draft, F. Ramezani; Writing—review & editing, R.J.C. Carbas, E.A.S. Marques and L.F.M. da Silva; Supervision, R.J.C. Carbas, E.A.S. Marques, and L.F.M. da Silva.

## Acknowledgments

The authors gratefully acknowledge the Portuguese Foundation for Science and Technology (FCT) for supporting the work presented.

## Conflict of Interest

The authors declared no potential conflicts of interest concerning the research, authorship, and publication of this article.

## Funding

The authors gratefully acknowledge the Portuguese Foundation for Science and Technology (FCT) for supporting the work presented here through the individual grants CEECIND/03276/2018 and 2021.07943.BD and Project No. PTDC/EME-EME/2728/2021, “New approaches to improve the joint strength and reduce the delamination of composite adhesive joints”.

## Data Availability Statements

Not Applicable.


## References


- [1] Karatas, M.A. and Gökkaya, H., A review on machinability of carbon fiber reinforced polymer (CFRP) and glass fiber reinforced polymer (GFRP) composite materials, *Defence Technology*, 14(4), 2018, 318-326.
- [2] Sahu, P. and Gupta, M.K., A review on the properties of natural fibres and its bio-composites: Effect of alkali treatment, *Proceedings of the Institution of Mechanical Engineers, Part L: Journal of Materials: Design and Applications*, 234(1), 2020, 198-217.
- [3] Zhou, M., Gu, W., Wang, G., Zheng, J., Pei, C., Fan, F. and Ji, G., Sustainable wood-based composites for microwave absorption and electromagnetic interference shielding, *Journal of Materials Chemistry A*, 8(46), 2020, 24267-24283.
- [4] Budzik, M.K., Wolfahrt, M., Reis, P., Kozłowski, M., Sena-Cruz, J., Papadakis, L., Nasr Saleh, M., Machalicka, K.V., Teixeira de Freitas, S. and Vassilopoulos, A.P., Testing mechanical performance of adhesively bonded composite joints in engineering applications: An overview, *The Journal of Adhesion*, 98(14), 2022, 2133-2209.
- [5] Nassiraei, H. and Rezadoost, P., Static capacity of tubular X-joints reinforced with fiber reinforced polymer subjected to compressive load, *Engineering Structures*, 236, 2021, 112041.
- [6] Nassiraei, H. and Rezadoost, P., Local joint flexibility of tubular T/Y-joints retrofitted with GFRP under in-plane bending moment, *Marine Structures*, 77, 2021, 102936.
- [7] Liu, B., Zhang, Q., Li, X., Guo, Y., Zhang, Z., Yang, H. and Yuan, Y., Potential advantage of thin-ply on the composite bolster of a bogie for a high-speed electric multiple unit, *Polymer Composites*, 42(7), 2021, 3404-3417.
- [8] Shishesaz, M., Ghamarian, A.H. and Moradi, S., Stress distribution in laminated composite tubular joints with damaged adhesive layer under torsion, *The Journal of Adhesion*, 99(6), 2023, 930-971.
- [9] Zou, G.P. and Taheri, F., Stress analysis of adhesively bonded sandwich pipe joints subjected to torsional loading, *International Journal of Solids and Structures*, 43(20), 2006, 5953-5968.
- [10] Shishesaz, M. and Tehrani, S., The effects of circumferential voids or debonds on stress distribution in tubular adhesive joints under torsion, *The Journal of Adhesion*, 96, 2020, 1396-1430.
- [11] Shishesaz, M. and Tehrani, S., Interfacial shear stress distribution in the adhesively bonded tubular joints under tension with a circumferential void or debond, *Journal of Adhesion Science and Technology*, 34(11), 2020, 1172-1205.
- [12] Zhou, X., Li, J., Qu, C., Bu, W., Liu, Z., Fan, Y. and Bao, G., Bending behavior of hybrid sandwich composite structures containing 3D printed PLA lattice cores and magnesium alloy face sheets, *The Journal of Adhesion*, 98(11), 2022, 1713-1731.
- [13] Guillamet, G., Turon, A., Costa, J., Renart, J., Linde, P. and Mayugo, J.A., Damage occurrence at edges of non-crimp-fabric thin-ply laminates under off-axis uniaxial loading, *Composites Science and Technology*, 98, 2014, 44-50.
- [14] Tserpes, K., Barroso-Caro, A., Carraro, P.A., Beber, V.C., Floros, I., Gamon, W., Kozłowski, M., Santandrea, F., Shahverdi, M., Skejic, D. and Bedon, C., A review on failure theories and simulation models for adhesive joints, *The Journal of Adhesion*, 98(12), 2022, 1855-1915.
- [15] Esmaeel, R.A. and Taheri, F., Stress analysis of tubular adhesive joints with delaminated adherend, *Journal of Adhesion Science and Technology*, 23(13-14), 2009, 1827-1844.
- [16] Esmaeel, R.A. and Taheri, F., Influence of adherend's delamination on the response of single lap and socket tubular adhesively bonded joints subjected to torsion, *Composite Structures*, 93(7), 2011, 1765-1774.
- [17] Sam-Daliri, O., Farahani, M. and Araei, A., Condition monitoring of crack extension in the reinforced adhesive joint by carbon nanotubes, *Welding Technology Review*, 91(12), 2019, 7-15.
- [18] Ghabeezi, P. and Farahani, M., Trapezoidal traction-separation laws in mode II fracture in nano-composite and nano-adhesive joints, *Journal of Reinforced Plastics and Composites*, 37(11), 2018, 780-794.





- [19] Ramezani, F., Simões, B.D., Carbas, R.J., Marques, E.A. and da Silva, L.F.M., Developments in Laminate Modification of Adhesively Bonded Composite Joints, *Materials*, 16(2), 2023, 568.
- [20] Akhavan-Safar, A., Ramezani, F., Delzendehrooy, F., Ayatollahi, M.R. and Da Silva, L.F.M., A review on bi-adhesive joints: Benefits and challenges, *International Journal of Adhesion and Adhesives*, 114, 2022, 103098.
- [21] Qin, Z., Yang, K., Wang, J., Zhang, L., Huang, J., Peng, H. and Xu, J., The effects of geometrical dimensions on the failure of composite-to-composite adhesively bonded joints, *The Journal of Adhesion*, 97(11), 2021, 1024-1051.
- [22] Ramezani, F., Nunes, P.D.P., Carbas, R.J.C., Marques, E.A.S. and da Silva, L.F.M., The joint strength of hybrid composite joints reinforced with different laminates materials, *Journal of Advanced Joining Processes*, 5, 2022, 100103.
- [23] Simões, B.D., Nunes, P.D., Ramezani, F., Carbas, R.J., Marques, E.A. and da Silva, L.F.M., Experimental and numerical study of thermal residual stresses on multimaterial adherends in single-lap joints, *Materials*, 15(23), 2022, 8541.
- [24] Shang, X., Marques, E.A.S., Machado, J.J.M., Carbas, R.J.C., Jiang, D. and Da Silva, L.F.M., A strategy to reduce delamination of adhesive joints with composite substrates, *Proceedings of the Institution of Mechanical Engineers, Part L: Journal of Materials: Design and Applications*, 233(3), 2019, 521-530.
- [25] Potter, K.D., Guild, F.J., Harvey, H.J., Wisnom, M.R. and Adams, R.D., Understanding and control of adhesive crack propagation in bonded joints between carbon fibre composite adherends I, Experimental, *International Journal of Adhesion and Adhesives*, 21(6), 2001, 435-443.
- [26] Mouritz, A.P., Review of z-pinned composite laminates, *Composites Part A*, 38(12), 2007, 2383-2397.
- [27] Ko, F.K. and Wan, L.Y., *Textile structural composites: from 3-D to 1-D fiber architecture. The structural integrity of carbon fiber composites: Fifty years of progress and achievement of the science, development, and applications*, Springer, 2017.
- [28] Sawyer, J.W., Effect of stitching on the strength of bonded composite single lap joints, *AIAA Journal*, 23(11), 1985, 1744-1748.
- [29] Hader-Kregl, L., Wallner, G.M., Kralovec, C. and Eysell, C., Effect of inter-ply on the short beam shear delamination of steel/composite hybrid laminates, *The Journal of Adhesion*, 95(12), 2019, 1088-1100.
- [30] Verpoest, I., Wevers, M., De Meester, P. and Declercq, P., 2.5 D-fabrics and 3D-fabrics for delamination resistant composite laminates and sandwich structures, *Sampe Journal*, 25(3), 1989, 51-56.
- [31] Dransfield, K., Baillie, C. and Mai, Y.W., Improving the delamination resistance of CFRP by stitching—a review, *Composites Science and Technology*, 50(3), 1994, 305-317.
- [32] Sihm, S., Kim, R.Y., Kawabe, K. and Tsai, S.W., Experimental studies of thin-ply laminated composites, *Composites Science and Technology*, 67(6), 2007, 996-1008.
- [33] Amacher, R., Cugnoni, J., Botsis, J., Sorensen, L., Smith, W. and Dransfeld, C., Thin ply composites: Experimental characterization and modeling of size-effects, *Composites Science and Technology*, 101, 2014, 121-132.
- [34] Arteiro, A., Catalanotti, G., Xavier, J., Linde, P. and Camanho, P.P., A strategy to improve the structural performance of non-crimp fabric thin-ply laminates, *Composite Structures*, 188, 2018, 438-449.
- [35] Kötter, B., Karsten, J., Körbelin, J. and Fiedler, B., CFRP thin-ply fibre metal laminates: Influences of ply thickness and metal layers on open hole tension and compression properties, *Materials*, 13(4), 2020, 910.
- [36] Wisnom, M.R., Khan, B. and Hallett, S.R., Size effects in unnotched tensile strength of unidirectional and quasi-isotropic carbon/epoxy composites, *Composite Structures*, 84(1), 2008, 21-28.
- [37] Kim, R.Y. and Soni, S.R., Experimental and analytical studies on the onset of delamination in laminated composites, *Journal of Composite Materials*, 18(1), 1984, 70-80.
- [38] Huang, C., He, M., He, Y., Xiao, J., Zhang, J., Ju, S. and Jiang, D., Exploration relation between interlaminar shear properties of thin-ply laminates under short-beam bending and meso-structures, *Journal of Composite Materials*, 52(17), 2018, 2375-2386.
- [39] Kupski, J., Zarouchas, D. and de Freitas, S.T., Thin-ply in adhesively bonded carbon fiber reinforced polymers, *Composites Part B: Engineering*, 184, 2020, 107627.
- [40] Camanho, P.P., Dávila, C.G., Pinho, S.T., Iannucci, L. and Robinson, P., Prediction of in situ strengths and matrix cracking in composites under transverse tension and in-plane shear, *Composites Part A: Applied Science and Manufacturing*, 37(2), 2006, 165-176.
- [41] Ramezani, F., Carbas, R.J., Marques, E.A. and da Silva, L.F.M., Study of Hybrid Composite Joints with Thin-Ply-Reinforced Adherends, *Materials*, 16(11), 2023, 4002.
- [42] Ramezani, F., Carbas, R.J., Marques, E.A., Ferreira, A.M. and da Silva, L.F.M., A study of the fracture mechanisms of hybrid carbon fiber reinforced polymer laminates reinforced by thin-ply, *Polymer Composites*, 44(3), 2023, 1672-1683.
- [43] Morgado, M.A., Carbas, R.J.C., Dos Santos, D.G. and Da Silva, L.F.M., Strength of CFRP joints reinforced with adhesive layers, *International Journal of Adhesion and Adhesives*, 97, 2020, 102475.
- [44] Campilho, R.D., De Moura, M.F.S.F. and Domingues, J.J.M.S., Modelling single and double-lap repairs on composite materials, *Composites Science and Technology*, 65(13), 2005, 1948-1958.
- [45] Machado, J.J.M., Marques, E.A.S., Campilho, R.D.S.G. and da Silva, L.F.M., Mode I fracture toughness of CFRP as a function of temperature and strain rate, *Journal of Composite Materials*, 51(23), 2017, 3315-3326.
- [46] Morgado, M.A., Carbas, R.J.C., Marques, E.A.S. and Da Silva, L.F.M., Reinforcement of CFRP single lap joints using metal laminates, *Composite Structures*, 230, 2019, 111492.
- [47] Ramezani, F., Carbas, R., Marques, E.A.S., Ferreira, A.M. and da Silva, L.F.M., Study on out-of-plane tensile strength of angle-ply reinforced hybrid CFRP laminates using thin-ply, *Mechanics of Advanced Materials and Structures*, 2023, 1-14.
- [48] Antunes, D.P.C., Lopes, A.M., Moreira da Silva, C.M.S., da Silva, L.F.M., Nunes, P.D.P., Marques, E.A.S. and Carbas, R. J. C., Development of a Drop Weight Machine for Adhesive Joint Testing, *Journal of Testing and Evaluation*, 49(3), 2021, 1651-1673.
- [49] Ghasbezi, P. and Farahani, M., A cohesive model with a multi-stage softening behavior to predict fracture in nano composite joints, *Engineering Fracture Mechanics*, 219, 2019, 106611.

## ORCID iD

Farin Ramezani  <https://orcid.org/0000-0003-3447-8515>

Ricardo J.C. Carbas  <https://orcid.org/0000-0002-1933-0865>

Eduardo A.S. Marques  <https://orcid.org/0000-0002-2750-8184>

Lucas F.M. da Silva  <https://orcid.org/0000-0003-3272-4591>



© 2023 Shahid Chamran University of Ahvaz, Ahvaz, Iran. This article is an open access article distributed under the terms and conditions of the Creative Commons Attribution-NonCommercial 4.0 International (CC BY-NC 4.0 license) (<http://creativecommons.org/licenses/by-nc/4.0/>).

**How to cite this article:** Ramezani F., Carbas R.J.C., Marques E.A.S., da Silva L.F.M. Study of Hybrid Composite Joints with Thin-ply-reinforced Adherends under High-rate and Impact Loadings, *J. Appl. Comput. Mech.*, 10(2), 2024, 260–271. <https://doi.org/10.22055/jacm.2023.44216.4181>

**Publisher's Note** Shahid Chamran University of Ahvaz remains neutral with regard to jurisdictional claims in published maps and institutional affiliations.

